GEOFIZIKA VOL. 31 2014

DOI: 10.15233/gfz.2014.31.6
Original scientific paper
UDC 551.509.32

Verification of WRF rainfall forecasts over India during monsoon 2010: CRA method

Ananda Kumar Das [1], *Mansi Bhowmick* [2], *P. K. Kundu* [3] *and S. K. Roy Bhowmik* [1]

[1] India Meteorological Department, Mausam Bhawan, New Delhi, India

[2] The University of Leeds, School of earth and Environment, Leeds, UK

[3] Jadavpur University, Department of Mathematics, Kolkata, India

Received 28 October 2013, in final form 2 September 2014

The WRF model forecast during monsoon season 2010 has been verified with daily observed gridded rainfall analysis with 0.5° spatial resolution. Firstly, the conventional neighborhood technique has been deployed to calculate common scores like mean error and root mean square error. Along with, widely used two categorical skill scores have been computed for seven different rainfall thresholds. The scores only found the general nature of the model performance and depicted the degradation of forecast accuracy exceeding moderate rainfall category of 7.5 mm. The object oriented Contiguous Rain Area method also has been considered for the verification of rainfall forecasts to gather more information about model performance. The method similarly has endorsed that the performance of the model degrades along with the increase in rainfall amount. But at the same time, the decomposition of mean square error has pointed out that the maximum error occurred due the shifting of rain object or event in the forecast compared to observation. The volume error contributes less as compared to pattern error in 24 hour forecasts irrespective of rainfall thresholds. But in 48 hour forecasts, their values are comparable and change along with rainfall threshold. During whole monsoon season, all contiguous rain areas in model forecasts have been searched over observed rainfall analyses applying best-fit criteria. For contiguous rain areas below 50 mm more than 70 percent match was found.

Keywords: contiguous rain area

1. Introduction

Forecasting of rainfall during Indian summer monsoon season is the most challenging task for numerical weather prediction models. As the rain bearing systems of monsoon embedded in large scale flow signify non-linear scale inter-

actions and varieties in physical process, their observed nature in terms of rainfall is still to be thoroughly studied. Therefore, verification of rainfall forecasts compared with observations during monsoon is always a matter of concern for the researcher. Many studies by several authors (e.g. Basu, 2005; Roy Bhowmik et al., 2006; Mandal et al., 2007; Roy Bhowmik and Durai, 2009) on rainfall verification over Indian peninsular region and its sub-regions during monsoon season have been carried out considering different time and horizontal scale during monsoon for different kinds of models. Verification studies (Das et al., 2008; Ashrit and Saji, 2010) in quantitative terms using categorical and continuous skill scores collectively portray inadequate picture for mesoscale forecasts. Categorical scores also could not bring reasonable picture for observed rainfall events with changing amount i.e. dimension (Hogan et al., 2010).

Within the scope of verification as recommended by WWRP/WGNE (World Weather Research Programme/Working Group of Numerical Experimentation; WMO, 2008), the verification of rainfall forecasts can be sought to improve forecast quality through better understanding of forecasts errors. There are various methods of verification alternative to point-wise comparison between forecast and observation. Applying three such different verification techniques for wind components (e.g. anomaly correlation, object-based verification and variance anomalies), Rife and Davis (2005) illustrated the benefit of high-resolution over coarse grid structure of the model in terms of temporal error variance and realistic nature of error growth. Newly modified neighborhood verification approach (e.g. fuzzy; Ebert, 2008, fractions skill scores; Roberts and Lean, 2008) are a bit superior to old type of the same class (e.g. root mean square error, mean error, correlation coefficient, skill scores and etc.; Theis et al., 2005) but give credit only to the close forecasts. As mentioned in the recommendations (WMO 2008), diagnostic methods give more in-depth information about the model performance. Simple methods using maps; time series; scatter plots; quantile-quantile or exceedance probability produce handy graphical results. But advance diagnostic methods have proven to be very much useful in evaluating deterministic models both in research and operational settings. Some examples include multi-scale spatial statistics, scale decomposition methods, field verification methods and object oriented methods. Harris et al. (2001) employed three methods of multiscale statistical analysis to assess model forecasts at high resolution for a convective storm using radar observations. Scale decomposition methods for precipitation forecasts define the intensity and scale of the errors e. g. intensity based scale separation (Casati et al., 2004). For objective evaluation of a regional ensemble forecasting system Kiel and Craig (2007) proposed a technique based on pyramidal matching algorithm. Object oriented verification methods e.g. Contiguous Rain Area (CRA) method (Ebert and McBride 2000; Grams et al., 2006), Method for Object-based Diagnostic Evaluation (MODE) by Davis et al. (2006) and Structure-Amplitude-Location (SAL) method (Wernli et al., 2008) are feature based model evaluation and address the skill of forecasts for epi-

sodic and localized phenomena. In addition, the object oriented verification methods are basically designed for rainfall verification at high resolution and thus applicable for the evaluation of mesoscale models during monsoon season.

In this paper, the quantitative verification over Indian region for a whole monsoon season has been completed for WRF-ARW model forecasts within cold-start frame-work of mesoscale assimilation system operational in India Meteorological Department (IMD). The study is basically based on CRA method described by Ebert and Gallus (2009). The method has been employed for the evaluation of WRF model forecasts along with rainfall observations at matching resolutions (temporal and spatial). Although, a detail insight about the characteristics of forecast errors may be gained after pursuing rigorous and repetitive experiments on the same forecasting system for several monsoon seasons.

2. Methodology

2.1. Model and data

The regional mesoscale analysis and forecasting system WRFDA is installed for real-time use in IMD, Delhi with its different components i.e. preprocessing program (WPS and REAL), and assimilation program (WRFDA), boundary condition update (update_bc) and forecasting model (WRF-ARW). The model is configured to run over a domain (Latitude: from 23.2° S to 46.2° N; Longitude: from 39.6° E to 120.5° E – shown in Fig. 1a) with 27 km horizontal resolution and 38 vertical eta levels up to 50 hPa pressure level at the top. Out of 38 vertical eta levels, approximately 12 levels are within planetary boundary layer (PBL) depth (considering average 3.0 km) although most of the time during monsoon season the convective boundary layer is predominant over the region. The processed observations (SYNOP, SHIP, METAR, also include additional surface Automatic Weather Station – AWS, TEMP, pilot balloon, AIREP, ACARS, atmospheric motion vectors and scatterometer wind from satellite and other conventional data from different sources) have been assimilated in WRFDA system to improve the first guess Global Forecast System (GFS) analysis (operational in IMD) within the model domain. The schematic diagram of WRFDA system is shown in Fig. 1b. The figure 1b represents three-dimensional variational assimilation in cold start mode. The modeling system has been utilized to generate two days forecasts during whole monsoon season of 2010. Accordingly, the WRFDA produced mesoscale analysis every day at each specified time (00 UTC). The update_bc component of WRFDA system also each time suitably updated boundary condition for the model. The model has then been integrated up to 51 hours. The WRF model has been configured with full physics (including cloud microphysics, cumulus, planetary boundary layer and surface layer parameterization) as well. The different physical parameterization schemes selected in WRF model have been represented in Tab. 1.

Table 1. WRF model configuration.

WRF model	ARW version 3.1.1
Domain and resolution	27 km (23.2°S to 46.2°N; 39.6°E to 120.5°E) 38 vertical eta levels
Microphysics	Lin et al. scheme
Radiation scheme (long-wave)	RRTM scheme
Radiation scheme (short-wave)	Dudhia's short wave radiation
Sfc layer physics	Monin-Obukhov scheme
Sfc layer parameterization	Thermal diffusion scheme
PBL parameterization	YSU scheme
Cumulus parameterization schemes	Betts-Miller-Janjic scheme

The verification experiments are framed according to the nature of available observations and forecast rainfall generated daily in IMD during monsoon 2010. As per conventional practice in IMD, the accumulation period of observed rainfall for a day is considered from 03 UTC of a day to next day 03 UTC. The observed (verification) analyses for rainfall generated in IMD (Rajeevan et al., 2005; Rajeevan and Bhate 2008, 2009) have been utilized at horizontal resolution (0.5°) within a box (Latitude: from 6.5° N to 38.5° N and Longitude: from 66.5° E to 100.5° E – shown in inner box of Fig. 1a) covering Indian region. The dataset of 0.5° × 0.5° resolution has been developed using quality controlled rainfall data from more than 3000 rain gauge stations over India (shaded region in Fig. 1a). They have utilized a well-tested interpolation technique (Shepard's method) to interpolate station data into regular grids with proper validation. The rainfall values at the grid points within shaded region of the verification domain (Fig. 1a) have been set from the 0.5° × 0.5° rainfall analysis and rest of the grid points of the domain have been filled with the interpolated rainfall values from TRMM (3B42V6.0 at 0.25° × 0.25° resolution) rainfall. The WRF-ARW forecast rainfall has been interpolated to 0.5° × 0.5° from its native 27 km resolution and accumulation period also have been matched with the observation. The verifications using neighborhood technique with two different approaches have been completed with the grid-point analyses and up scaled forecast rainfall for whole India region. In first approach general scores like mean error (*ME*), mean square error (*MSE*) and root mean square error (*RMSE*) have been computed along with widely used two categorical skill scores (threat score and equitable threat score) for seven rainfall thresholds. In next approach, objected oriented CRA method has been employed for verification over whole India region.

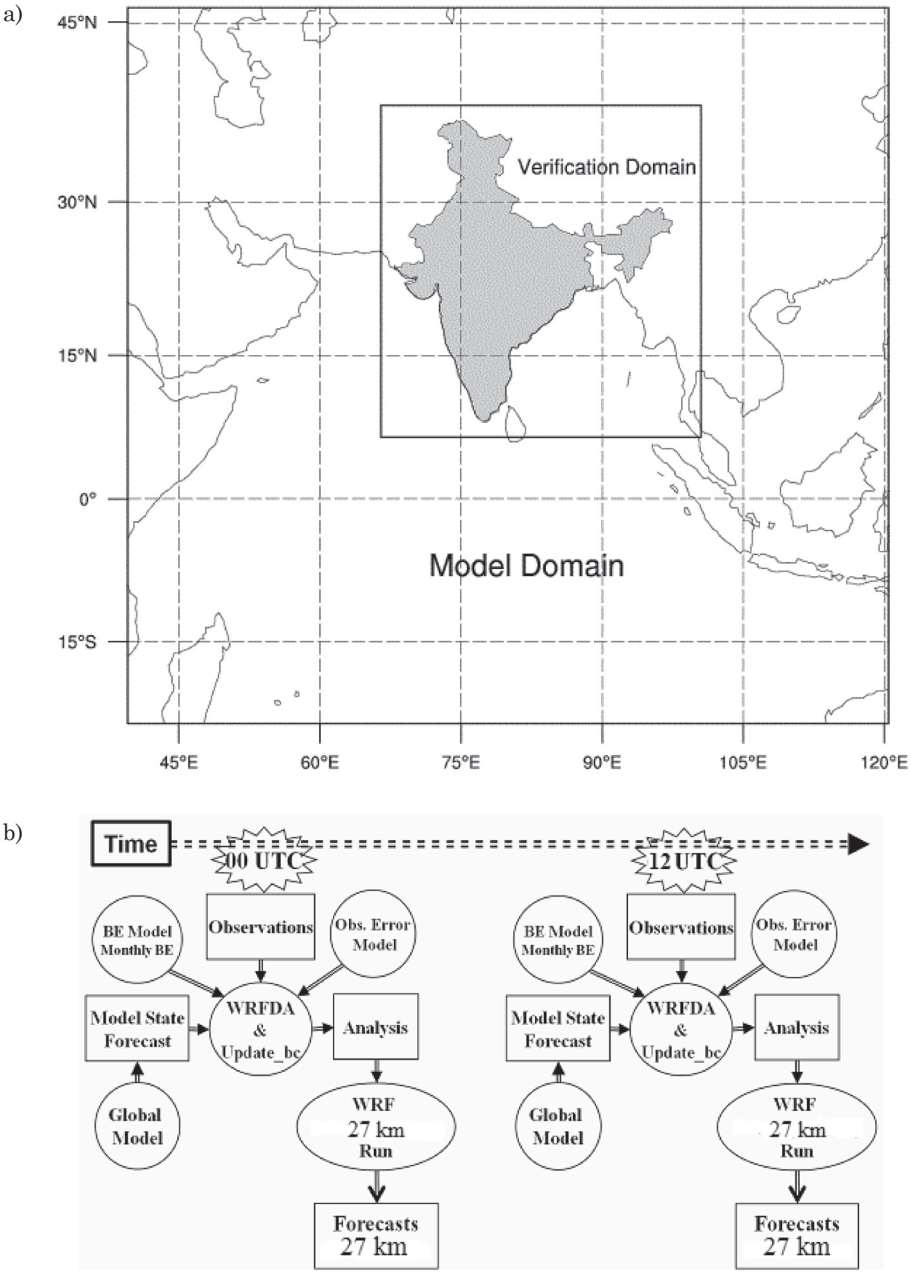

Figure 1. (*a*) Domain of WRF model with 27 km resolution (model domain) and inner box shows the area of verification domain where shaded area represents data coverage of 0.5°×0.5° rainfall analysis in IMD. (*b*) The schematic diagram of the assimilation procedure of WRFDA-WRF-ARW system.

2.2. CRA method

The CRA method utilized in this study has been developed following the algorithm of the technique described in a study by Ebert and Gallus (2009) but the realization of the working steps have to be formulated according to the distinct features and characteristics of available observed and forecast rainfall over the region during whole monsoon season. The CRA method has been employed judiciously for a rainfall threshold on the basis of the nature and sizes the defined objects over the region. At the same time, the object oriented method focus on the ambiguity in performance analysis through categorical scores for different thresholds.

The categorical verification scores for rainfall have been utilized to evaluate model performance. The different rainfall categories are defined on the basis of

Table 2. Classification of rainfall based on intensity.

Descriptive term used	Category	Rainfall amount in mm
No rain	I	0.0
Very light rain	II	0.1–2.4
Light rain	III	2.5–7.5
Moderate rain	IV	7.6–35.5
Rather heavy	V	35.6–64.4
Heavy rain	VI	64.5–124.4
Very heavy rain	VII	124.5–244.4
Extremely heavy rain	–	**≥244.5**
Exceptionally heavy rain		When the amount is a value near about the highest recorded rainfall at or near the station for the month or season.

Table 3. Average sizes of CRA for different rain thresholds converted to equivalent square.

Rainfall thresholds in mm per day	Average no of adjacent points from 0.5°×0.5° gridded data	Average size of CRA converted to equivalent square area
2.4	1974	22°×22°
7.5	876	15°×15°
21.5	184	7°×7°
35.5	68	4°×4°
50	46	3°×3°
64.5	38	2.5°×2.5°

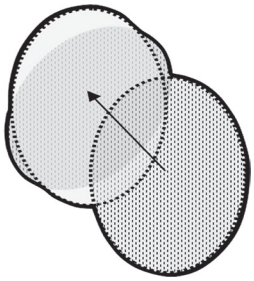

Figure 2. CRA formed by the overlap of the forecast (region outlined by dashed line), which has original position at lower right position and final best-fit at upper left position with the observations (darker region). The small dotted region shows the CRA before translation of the forecast in the direction of the arrow. The heavy black outline shows the template for which verification statistics are computed.

the classification used in India Meteorological Department (described in Tab. 2). In this document, last two categories above very heavy rain class are not considered for the verification purpose as their occurrences are limited over a region with comparatively small spatial coverage throughout monsoon season 2010. The underestimation and poor forecasting of heavy rainfall events by numerical models is also a fact already been depicted by previous studies over the region (Das et al., 2008; Durai et al., 2010). Rainfall categories 2.4 mm and 7.5 mm have not been considered as the defined object (CRA) for these thresholds are too big to be considered in CRA method. The average sizes of the objects for different rainfall thresholds are tabulated in Tab. 3. The rainfall over Indian region during monsoon season most widespread and moreover rainfall analysis with 0.5° resolution could not depict discontinuity (if exists) within spatial distribution of rainfall. As a result, on average daily template of computed CRAs for 2.4 mm and 4.6 mm rain thresholds cover large areas.

In Fig. 2, the schematic view of CRA formation has been shown which has been thoroughly described in the article by Ebert and Gallus (2009). The figure is self explanatory with the representation of forecast, observed field and merged fields and it has been reproduced from the study mentioned above. The detail of method followed in this study is already described in the referred research paper. Only, the working implementation of the CRA method for the present study has been formulated in the following steps:

(i) Both observed and forecast rainfall fields are merged by retaining greater value of rainfall at certain grid point.

(ii) Extract the grids points with rain value greater than or equal to a given threshold based on considered rainfall categories.

(iii) Flood fill (seed fill) algorithm has been employed to find contiguous rain area (a collection of grid points exceeding threshold adjacent to each other) from extracted grid points in previous step (ii).

(iv) The rectangular template from observed field according to horizontal span of the CRA zone (maximum and minimum value of latitude and longitude) has been defined for further procedural steps.

(v) Sufficiently large search domain from forecast field has been created by extending the boundaries of the previously selected rectangular template in all the four sides. In present study, 1.5 times of observed template length and breadth have been enlarged to set the search domain. But the maximum horizontal extension has not crossed the limit less than or equal to 5 degree on each side.

(vi) Consequently, observed template has been displaced over search domain of forecast field till best match criterion has been fulfilled i.e. maximum spatial correlation coefficient has been reached.

(vii) Only those rain grid point information has been retained for which simultaneously both defined criteria (spatial correlation coefficient ≥ 0.3 and Mean Squared Error <1600 mm^2) has been satisfied.

(viii) Finally according to Ebert and McBride (2000), total mean square error in terms of percentage displacement, volume and pattern has been decomposed as

$$MSE_{total} = MSE_{displacement} + MSE_{volume} + MSE_{pattern.}$$

The decomposition procedure computes the displacement component as the difference in the mean squared error before and after shifting the forecast, the volume error as the bias in mean intensity, and the pattern error as a residual.

$MSE_{displacement} = MSE_{total} - MSE_{shifted}$, $MSE_{volume} = \left(\bar{F} - \bar{X}\right)^2$ and $MSE_{pattern} = MSE_{shifted} - MSE_{volume}$ where $\bar{F}$ and $\bar{X}$ are the mean forecast and observed values after the shift.

(ix) But for the cases where $MSE_{total} < MSE_{shift}$ i.e. $\%MSE_{displacement}$ is negative the modified formula from Murphy (1995) have been utilized.

$MSE_{total} = \left(\bar{F} - \bar{X}\right)^2 + \left(s_x - r\, s_F\right)^2 + \left(1 - r^2\right) {s_F}^2$, where s_F and s_x are the standard deviations for forecast and observed values respectively; and r is the original spatial correlation between the forecast and observed rain. Shifting the forecast template location improves its correlation with the observations to r_{opt}. The decomposition formula now become

$MSE_{displacement} = 2\, s_F\ s_x\, (r_{opt} - r)$

$MSE_{volume} = \left(\bar{F}' - \bar{X}'\right)^2$ and $MSE_{pattern} = 2\, s_F\ s_x\, (1 - r_{opt}) + (s_F\ -\ s_x)^2$.

In the next section, as an example, one rainfall object of a selected day has been considered to describe the method. The functional steps (i) to (ix) described above has been followed for the computation of error statistics. After a threshold has been set, the templates for observed, forecasted and combined CRA have been found out from their spatial distribution of rainfall over grid points. The

error partitions along with total error have been computed using the formula mentioned in step (viii) and (ix).

The all steps similarly have been employed separately for all CRAs of a day and for a certain threshold. Then the average statistics of CRAs for all days during whole monsoon season has been worked out to produce overall performance of model forecasts for that threshold. The performance statistics has been computed separately for different thresholds.

The matching criteria have been set to find the matches for the observed CRAs for a certain threshold. The specific observed object has been searched over respective forecasts and search has been continued as long as the maximum value of spatial correlation coefficient ≥ 0.4 (which statistically significant with level of significance 0.05 for a template having minimum of 20 points). As soon as the match is found for an observed object, the shift of respective forecast object has been computed from the initial and final positions of center of mass. When the matching criteria have not been satisfied for a certain observed CRA, the object is considered to be missed in the forecast. During the entire season, the match or miss statistics of all observed CRAs have been computed for different rainfall thresholds.

3. Results and discussion

3.1. Verification scores for rainfall

Verification of forecast rainfall with observed analysis has been done for Indian region considering whole monsoon period JJAS 2010 on the basis of standard scores such as *RMSE*, *ME*, *MSE* which has been computed and summarized for day 1 (27 hour) and day 2 (51 hour) forecasts. The scores mentioned above are computed daily taking average over the region to show time series of the errors in Fig. 3. The model forecast do not show any kind of feature in its performance during whole monsoon season rather portray random characteristics. Over all, the rainfall is overestimated in day 1 (~ 5 mm) and the overestimation is reduced in day 2 forecast (~ 2.0 mm) although there is significant improvement in *RMSE*. The model errors (*MSE* and *RMSE*) vary in day to day forecasts and systematic contribution in the error is less compared to its randomness.

Most common categorical skill scores (e.g. threat score and equitable threat score) for seven different rainfall categories have also been computed to evaluate the model performance in predicting rainfall over the region.

Although, model produce positively biased rainfall over every region throughout the season, the small values of mean error compared to *MAE* and *RMSE* depict the randomness of the error. The errors also enhances over the region of higher rainfall e.g. west-coast and north-eastern states. The order of errors does not portray any significant differences between different forecast lengths and specifically, day 2 have little higher values compared to day 1.

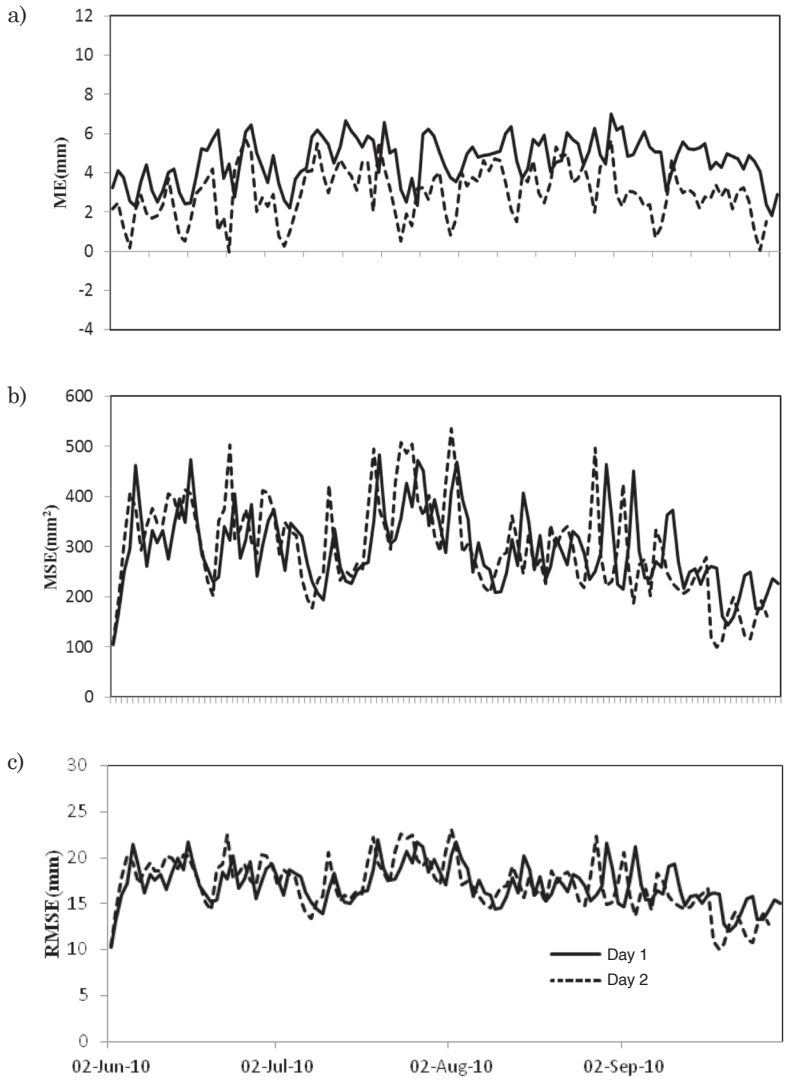

Figure 3. Errors in rainfall forecasts averaged over whole India region. (*a*) mean error (*ME*), (*b*) mean square error (*MSE*) and (*c*) root mean square error (*RMSE*).

In this document, the description has been limited to two specific categorical skill scores critical success index (*CSI*) and Gilbert Skill Score (*GSS*) commonly known as threat score and equitable threat score respectively for whole India. The *CSI* for seven threshold valued of rainfall masked over whole Indian domain shown in Fig. 4 depicted well-known characteristics of the score. The *CSI* score

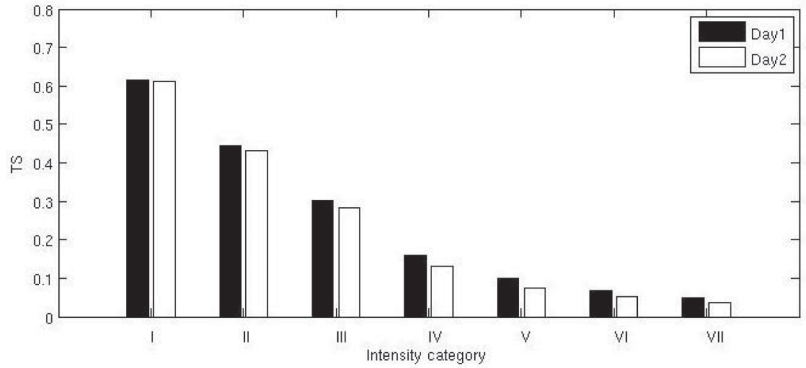

Figure 4. Threat scores at different rainfall categories in rainfall forecasts averaged over whole India region.

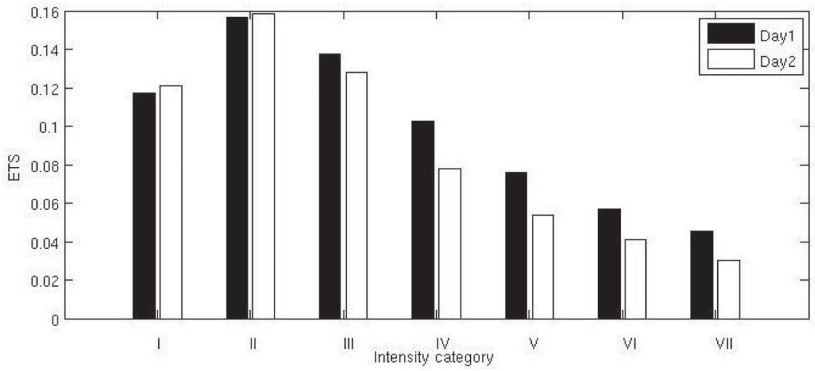

Figure 5. Equitable threat scores at different rainfall categories in rainfall forecasts averaged over whole India region.

degraded as with an increase in rainfall intensity. Performance of the model is below per for rainfall threshold above 35.5 mm. *GSS* score also suggests similar information (Fig. 5). *GSS* approaches to zero (no skill value) as rainfall amount rises above 35.5 mm. Although the values of the score far below 1.0 associated with correct forecast, the *GSS* score sometimes portray inadequate picture about the model performance at high resolution and the scores attest to the ability of phase correction and filtering over scales are necessary (Bousquet et al., 2006). As usual, model provides best performance in predicting rain and no-rain events (considering threshold of 0.1 mm). These two scores over whole India region signify that the model perform below an acceptable quality above moderate (7.5 mm) rainfall amount which is also in agreement with other previous verification studies with models over the region (Ashrit and Saji, 2010; Mandal et al., 2007).

The mean error, root mean square error gives performance measure of the model in absolute sense and do not ensure the specific nature of the model forecasts over the region. Categorical skill scores have victimized the model forecasts with double penalty as the model could not forecast rainfall events location (grid coverage) with absolute accuracy. The model forecasts have been exerting more errors added with the inaccuracy in pattern and intensity of rainfall. Therefore in the next section the results of verification with an object oriented method have been discussed.

3.2. Verification with CRA method

The observed and forecast and merger templates for a selected CRA on 30 July 2010 have been shown in Fig. 6. The solid outline in all panels shows the merged template crossing a threshold of 35.5 mm rainfall. Figures 6a and 6b represent the observed and forecast fields. The respective center of masses for both templates are located and marked with circle and C inside the shaded region of exceeding threshold rainfall. The details of template characteristics are given in Tab. 4. It is clearly seen that the major error occurs due to the displacement of the rainfall event in the forecast. Volume error does not show any major con-

Table 4. Template characteristics for the selected CRA on 30 July 2010.

Template characteristics	Observed CRA	Forecast CRA
Number of grid points	30	52
Location center	18.61° N, 80.41° E	19.14° N, 81.49° E
Mean rainfall	21.76 mm	30.98 mm
Rain maximum	125.8 mm	99.5 mm
Rain volume	3133.7 mm	4461.5 mm
RMSE	Comparisons of observed and forecast rainfall over same grid have been conducted and the scores and values in right column have been calculated.	52.68 mm before shift 31.89 mm after shift
Correlation coefficient		–0.3 before shift 0.7 after shift
Vector displacement/shift		1.2°
Latitude displacement/shift		–0.53°
Longitude displacement/shift		–1.08°
Mean Square Error		2774.8 sq. mm before shift 1017.1 sq. mm after shift 63.36 % for displacement 1.53 % for volume 35.12 % for pattern

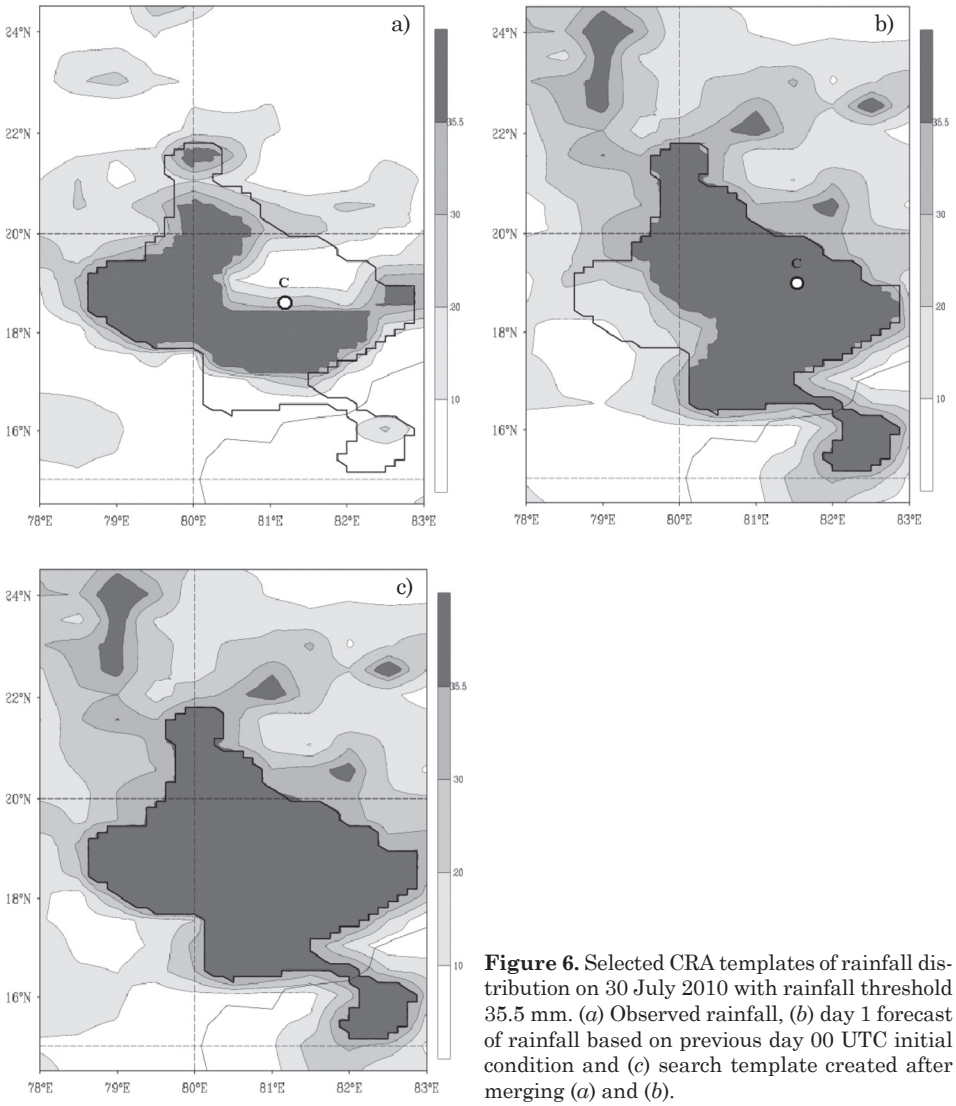

Figure 6. Selected CRA templates of rainfall distribution on 30 July 2010 with rainfall threshold 35.5 mm. (*a*) Observed rainfall, (*b*) day 1 forecast of rainfall based on previous day 00 UTC initial condition and (*c*) search template created after merging (*a*) and (*b*).

tribution while the best-fit criteria are fulfilled to cope up with displacement of the forecast compared to observed field. After the shifting of the templates to match the best-fit criteria the total error is significantly reduced which has been reflected in the values of *RMSE* (reduced from ~ 52 mm to 31 mm) and correlation coefficient (increased from –0.3 to 0.7). The extension of the study for all days of the season, the similar approach has been followed for all other individual CRAs found for a specific rainfall threshold in each day.

The experimentation has been conducted for the model forecasts with different thresholds to determine the minimum size of the CRA for certain category of rainfall. The variation in the number of CRA detected within the forecast and observed rainfall distribution during the season have been noticed as the minimum number of grid point changes. Figures 7 and 8 show that the number of CRA for all thresholds increases steadily with an increase in grid points for both day 1 and day 2 forecasts respectively. As we restrict the size of CRA with a number specified small number of grid points, the bigger rainfall area exceeding certain rainfall threshold splits up. Alongside, for small CRA over the specific region the selection of best match between observation and forecast is also difficult. The larger size also restricts to put best-fit criteria in a rather stringent manner. Although, the slope and number of CRA are not same for day 1 and day 2, but their overall nature is same for each threshold. The number of CRA in-

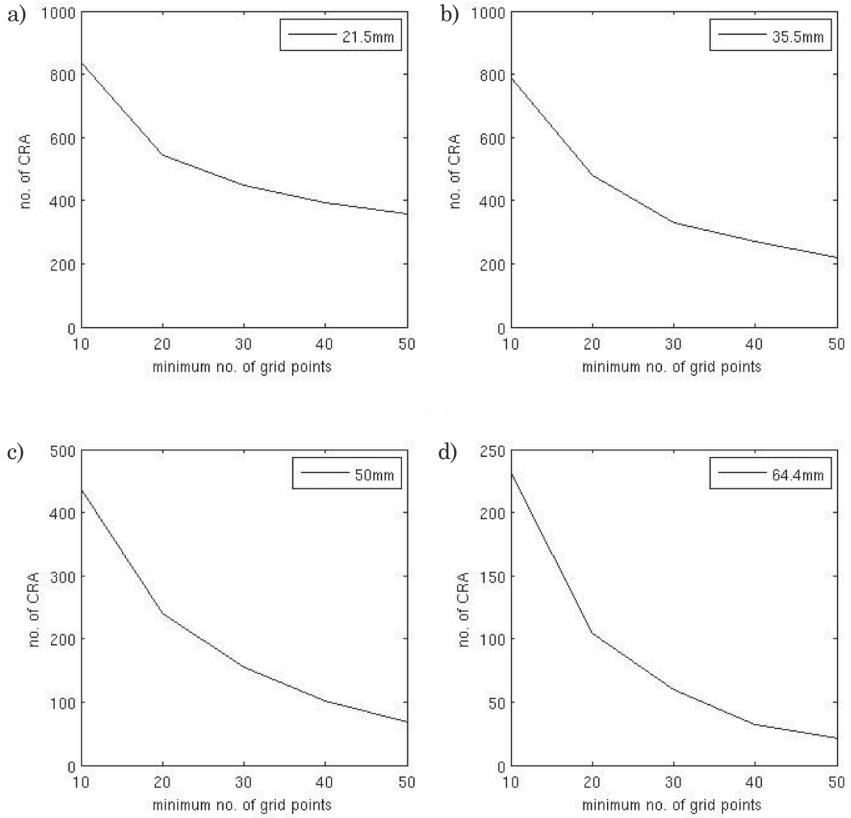

Figure 7. Variation in numbers of CRA at day 1 forecasts over whole India domain during the season with varying thresholds in rainfall amount and number of grid points in a CRA. (*a*) for 21.5 mm (*b*) 35.5 mm (*c*) 50 mm and (*d*) 64.4 mm rainfall thresholds.

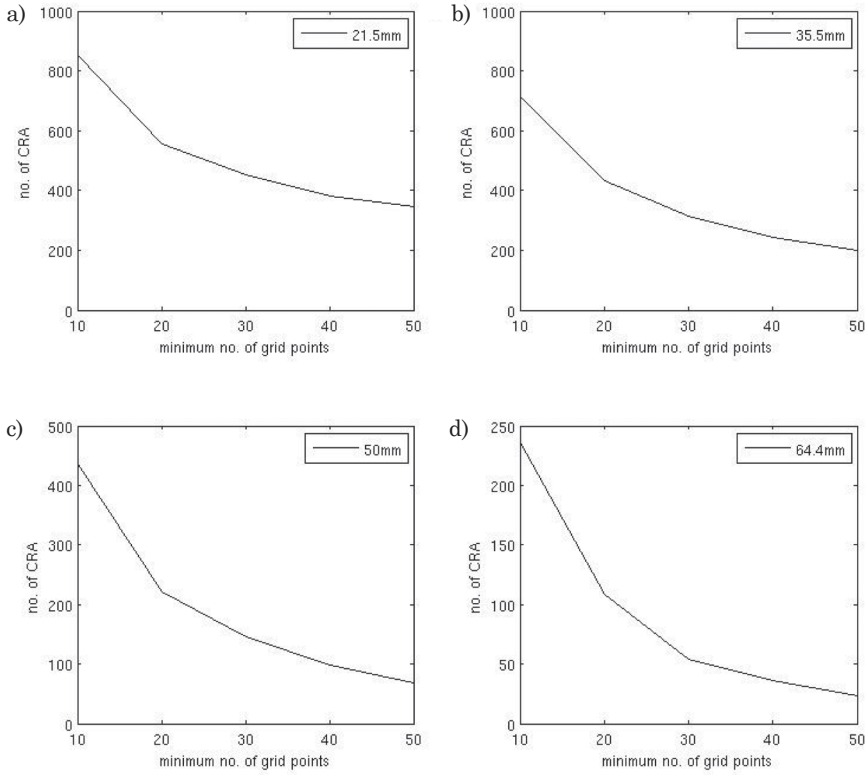

Figure 8. Same as Fig. 7, but for day 2 forecasts.

creases rapidly as the number grid points drops below 20 for all thresholds. When the minimum size of CRA is set above 20 number of grid points, the number of CRA decreases slowly for all categories. Therefore, for all rain thresholds, a common optimal size has been selected based on the curves in Figs. 7 and 8. The computation has been completed throughout all days of the season for those CRAs with a minimum size containing at least 20 grid points.

The figures 9 and 10 depicted the decomposition of *MSE* in day 1 and day 2 rainfall forecasts respectively for different thresholds during the season. The CRAs are stenciled separately for four different thresholds in a day and every individual CRA has been considered to make a match between observed and forecast fields. The forecast error for each CRA has been computed with three partitions i.e. displacement, pattern and volume errors. The mean value has been computed considering all CRAs for a certain threshold irrespective of their locations and the days of occurrence.

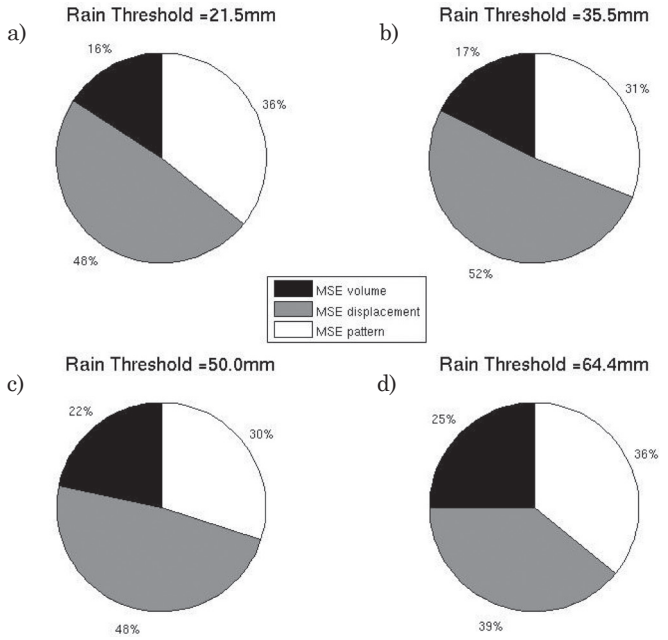

Figure 9. Pie chart of volume, displacement and pattern mean square errors in day 1 forecasts for different rainfall thresholds for (*a*) 21.5 mm (*b*) 35.5 mm (*c*) 50.0 mm and (*d*) 64.4 mm.

The figure 9 represents the seasonal error partitions of day 1 forecasts for four rain thresholds. Looking at the pie charts it is clear that the maximum error is due to displacement irrespective of rainfall amount. The distinct similarity has also been found for day 2 forecasts in Fig. 10. In case of day 1 forecasts, the contribution of pattern mismatch is always found to be greater than volume error for every rain threshold but for day 2 forecasts the relation between the partitions varies with rain threshold. In other words, the day 1 forecasts of the model maintain consistent relations between three components of *MSE* for all rain thresholds. The least error occurred due to rain intensity estimation whereas the highest error values arise because of displacement and the corresponding errors out of distribution-pattern mismatch lie in between them. The similar behavior has not been portrayed by day 2 forecasts. The volume and pattern errors nearly have similar significance within total forecast error for two intermediate rain thresholds (35.5 and 50 mm) but they behave randomly for other two. This illustrates the fact that the model forecasts loose coherence between structure and intensity going from day 1 to day 2 for certain CRAs. Thorough inspections yield that the volume error shows a little increasing trend with rainfall amount. This implicates that the model has comparatively poor skill for higher rainfall amount. But, this obviously does not provide any information about natural bias as the displacement error plays the crucial role to nullify any

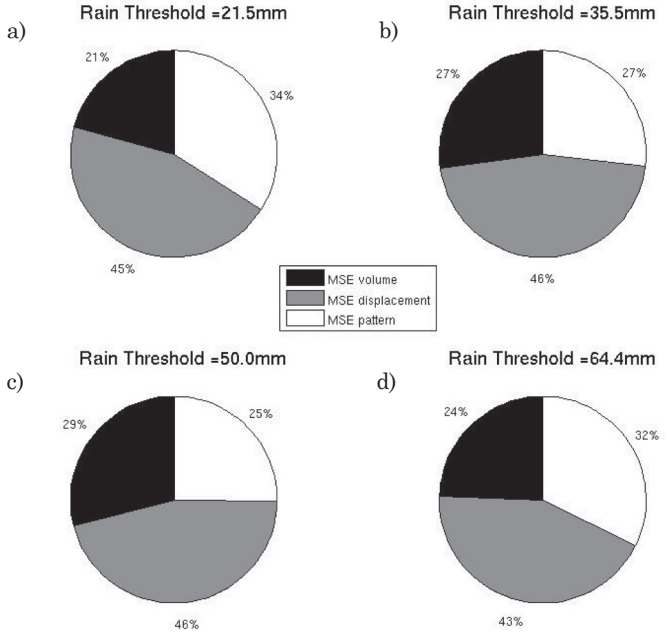

Figure 10. Same as Fig. 9, but for day 2 forecasts.

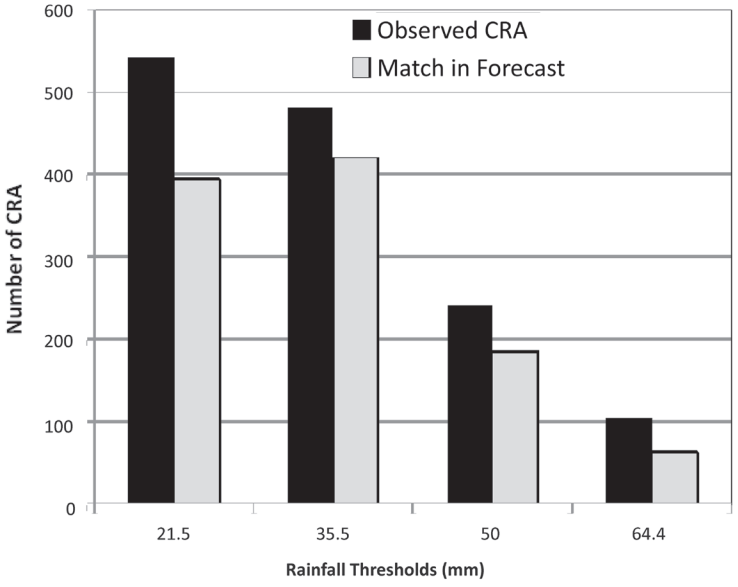

Figure 11. Number of observed CRA and number matches found in the day 1 forecasts for different thresholds of rainfall.

Table 5. Percentage of matches between observed CRA and forecasts for different thresholds of rainfall.

Rainfall threshold category (mm)	Match in forecasts (%)		Average linear displacement in forecasts (degree)	
	Day 1	Day 2	Day 1	Day 2
21.5	72.6	69.0	2.74	2.92
35.5	**87.3**	**80.8**	2.72	2.98
50.0	76.7	70.6	2.64	2.93
64.4	59.6	56.9	2.19	2.56

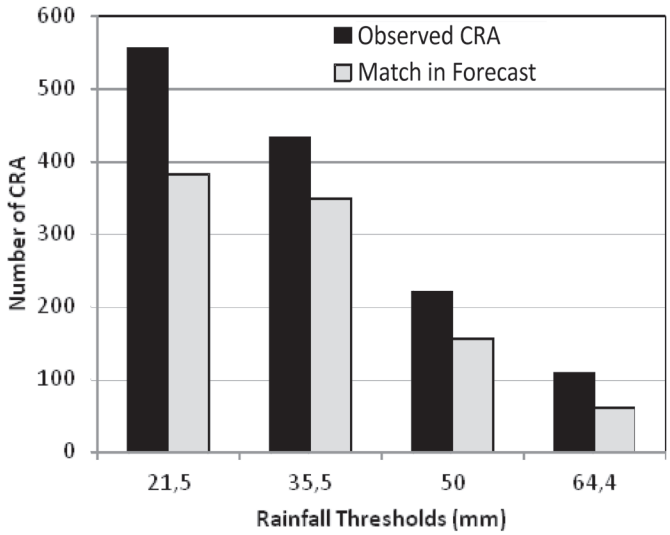

Figure 12. Same as Fig. 11, but for day 2 forecasts.

such bias in a random way. The major share of displacement error also shows an increase from 21.5 mm to 35.5 mm threshold but decreases thereafter in both forecasts hours (day 1 and 2).

The summary of match between observed and forecast CRAs are displayed in Figs. 11 and 12 for day 1 and day 2 forecasts respectively. Both figures show that the number of matches reduces along with the increase in rainfall. First two columns in Tab. 5 also summarize the percentage of matches found in day 1 and day 2 forecasts for different thresholds. It is also obvious that during whole season, the day 1 forecast of the model shows the superiority over day 2 for each category. The figures also show that the match percentage is higher at 35.5 mm

category compared 21.5 mm although total number of observed CRA decreases considerably.

The average linear displacement of the center of mass of forecast CRAs from their corresponding matches in observation has been computed for each 4 rain thresholds. The right most 2 columns in Tab. 5 are showing the average displacement of CRAs in degree (latitude and longitude combined). It is found that the order of average linear shift does not change drastically with rain intensity but a little increase has been found from day 1 to day 2. The seasonal mean displacement of rain object shows a marginal reduction with increasing rain amount. It does not have larger significance in statistical sense as the computation of mean have considered comparatively large number of CRA for lower thresholds (number of CRA falls with an increase in rain intensity shown in Figs. 7 and 8). Also, the average size of rain objects also shrinks for higher amount which in turn produce less error in locating the center of mass of each CRA compared to lower threshold.

4. Conclusion

The present study attempted to utilize the strength of the object oriented CRA method for rainfall verification to get an insight of the forecast error in terms of displacement, pattern and volume. The common verification scores like ME and RMSE along with categorical skill scores could bring out a few facts regarding model performance such as

(i) The errors in rainfall forecasts are random in nature but overall overestimation has been found during the whole season which is marginally reduced in day 2 forecast from day 1.

(ii) Categorical skill scores show that the model performance declines beyond acceptable limit exceeding moderate rainfall category.

(iii) Model performed poorly for heavy rainfall categories which have also been found in previous studies.

But, an insight in the model performance has been achieved applying CRA method and decomposed MSE have explained the comparative error contribution amongst displacement, pattern and volume. An example with a selected CRA within the season has shown that if the forecast CRA has been shifted to alleviate the error due to displacement the decrease in total errors have been accorded. The following facts have been brought out after using the specific object oriented verification.

(i) The model performance has shown evident decline in model performance with time and also with increasing rainfall intensity.

(ii) Still, the match between observed and forecast CRAs is above 70 percent when best-fit criteria have been deployed up to 50 mm rainfall threshold during the season and over whole India.

(iii) The displacement error has the major share within total MSE irrespective of forecast duration or rainfall threshold.

(iv) The day 1 forecasts of the model are more consistent in terms of the relative amplitudes of three different partitions of total MSE, but the regularity diminishes in day 2 forecasts.

(v) The mean displacement (shifting) of forecast CRA from the respecting match in observed field does not vary significantly with rain intensity but a certain increase have been noticed from day 1 to day 2 forecast.

The study only shows the beneficial use of CRA method for the verification of mesoscale forecasts. The CRA verification using rainfall analyses with higher horizontal and temporal resolution is expected to be more critical about model performance. Furthermore, the future studies over different geographical regions to realize the dependency of model performance over spatial heterogeneity. Different spells (active or subdued) of several monsoon seasons may also be studied to bring out specific nature of the model forecasts over temporal scales.

Acknowledgement – Authors are grateful to the Director General of Meteorology, India Meteorological Department for providing all facilities to carry out this research work. Authors acknowledge NCAR, USA for the support and sharing of the community code of WRF modeling system along with assimilation component WRFDA. The key research paper by Ebert and Gallus (2009) became immense help to this study and authors are thankful to them.

References

Ashrit, R., and Saji, M. (2010): Mesoscale model forecast verification during monsoon 2008, *J. Earth Syst. Sci.*, **119**, 417–446, DOI: 10.1007/s12040-010-0030-9.

Basu, B. K. (2005): Some characteristics of model-predicted precipitation during the summer monsoon over India, *J. Appl. Meteorol.*, **44**, 324–339, DOI: 10.1175/JAM-2198.1.

Bousquet, O., Lin C. A. and Zawadzki, I. (2006): Analysis of scale dependence of quantitative precipitation forecast verification: A case-study over the Mackenzie river basin, *Q. J. R. Meteor. Soc.*, **132**, 2107–2125, DOI: 10.1256/qj.05.154.

Casati, B., Ross G. and Stephenson, D. B. (2004): A new intensity-scale approach for the verification of spatial precipitation forecasts, *Meteorol. Appl.*, **11**, 141–154, DOI: 10.1017/S1350482704001239.

Das, Someshwar, Ashrit, R., Iyengar, G. R., Saji, M., Das Gupta, M., George, J. P., Rajagopal, E. N. and Dutta, S. K. (2008): Skills of different mesoscale models over Indian region during monsoon season: Forecast errors, *J. Earth Syst. Sci.*, **117**, 603–620, DOI: 10.1007/s12040-008-0056-4.

Davis, C., Brown B. and Bullock, R. (2006): Object-based verification of precipitation forecasts. Part I: Methodology and application to mesoscale rain areas, *Mon. Wea. Rev.*, **134**, 1772–1784, DOI: 10.1175/MWR3145.1.

Durai, V. R., Roy Bhowmik, S. K. and Mukhopadhyay, B. (2010): Performance evaluation of precipitation prediction skill of NCEP global forecasting system (GFS) over Indian region during summer monsoon 2008, *Mausam*, **61**, 139–154.

Ebert, E. E. and McBride, J. L. (2000): Verification of precipitation in weather systems: Determination of systematic errors, *J. Hydrol.*, **239**, 179–202, DOI: 10.1016/S0022-1694(00)00343-7.

Ebert, E. E. (2008): Fuzzy verification of high-resolution gridded forecasts: A review and proposed framework, *Meteorol. Appl.*, **15**, 51–64, DOI: 10.1002/met.25.

Ebert, E. E. and William, A. G. Jr., (2009) Toward better understanding of the contiguous rain area (CRA) method for spatial forecast verification, *Wea. Forecasting*, **24**, 1401–1415, DOI: 10.1175/2009WAF2222252.1.

Grams, J. S., Gallus Jr., W. A. Koch, S. E. Wharton, L. S., Loughe A. and Ebert, E. E. (2006): The use of a modified Ebert–McBride technique to evaluate mesoscale model QPF as a function of convective system morphology during IHOP 2002, *Wea. Forecasting*, **21**, 288–306, DOI: 10.1175/WAF918.1.

Harris, D., Foufoula-Georgiou, E., Droegemeier, K. K. and Levit, J. J. (2001): Multiscale statistical properties of a high-resolution precipitation forecast, *J. Hydrometeor.*, **2**, 406–418, DOI: 10.1175/1525-7541(2001)002<0406:MSPOAH>2.0.CO;2.

Hogan, R. J., Ferro, C. A. T., Jolliffe, I. T. and Stephenson, D. B. (2010): Equitability revisited: Why the 'equitable threat score' is not equitable, *Wea. Forecasting*, **25**, 710–726, DOI: 10.1175/2009WAF2222350.1.

Keil, C. and Craig, G. C. (2007): A displacement-based error measure applied in a regional ensemble forecasting system, *Mon. Wea. Rev.*, **135**, 3248–3259, DOI: 10.1175/MWR3457.1.

Mandal, V., De, U. K. and Basu, B. K. (2007): Precipitation forecast verification of the Indian summer monsoon with intercomparison of three diverse regions, *Wea. Forecasting*, **22**, 428–443, DOI: 10.1175/WAF1010.1.

Murphy, A. H. (1995): The coefficients of correlation and determination as measures of performance in forecast verification, *Wea. Forecasting*, **10**, 681–688, DOI: 10.1175/1520-0434(1995)010<0681:TCOCAD>2.0.CO;2.

National Center for Atmospheric Research, Boulder, Colorado, USA (2013): *The NCAR Command Language (Version 6.0.0)* [Software]. UCAR/NCAR/CISL/VETS. DOI: 10.5065/D6WD3XH5.

National Center for Atmospheric Research, Mesoscale & Microscale Meteorology Division, Boulder, Colorado, USA (2011): *WRF ARW Version 3 Modeling System User's Guide*, available at http://www.mmm.ucar.edu/wrf/users/docs/arw_v3.pdf

Rajeevan, M., Bhate, J., Kale, J. D. and Lal, B. (2005): Development of a high resolution daily gridded rainfall data for the Indian region. *IMD Met Monograph Climatology*, 22/2005, 26 pp, available at ftp://squall.met.fsu.edu/LAU/070108_1446/doc/ref_report.pdf.pdf

Rajeevan, M. and Bhate, J. (2008): A high resolution daily gridded rainfall data set (1971–2005) for mesoscale meteorological studies, *NCC (9) Research Report*. India Meteorological Department, Pune, 14v pp, available at http://www.imdpune.gov.in/ncc_rept/RESEARCH%20REPORT%209.pdf

Rajeevan, M. and Bhate, J. (2009): A high resolution daily gridded rainfall dataset (1971–2005) for mesoscale meteorological studies, *Current Science*, **96**, 558–562.

Rife, D. L. and Davis, C. A. (2005): Verification of temporal variations in mesoscale numerical wind forecasts, Mon. Wea. Rev., **133**, 3368–3381, DOI: 10.1175/MWR3052.1.

Roberts, N. M. and Lean, H. W. (2008): Scale-selective verification of rainfall accumulations from high-resolution forecasts of convective events, *Mon. Wea. Rev.*, **136**, 78–97, DOI: 10.1175/2007MWR2123.1.

Roy Bhowmik, S. K. and Durai, V. R. (2009): Application of multimodel ensemble techniques for real time district level rainfall forecasts in short range time scale over Indian region, *Meteorol. Atmos. Phys.*, **106**, 19–35, DOI: 10.1007/s00703-009-0047-2.

Roy Bhowmik, S. K., Joardar, D. and Hatwar, H. R. (2006): Evaluation of precipitation prediction skill of IMD operational NWP system over Indian monsoon region, *Meteorol. Atmos. Phys.*, **95**, 205–221, DOI: 10.1007/s00703-006-0198-3.

Theis, S. E., Hense, A. and Damrath, U. (2005): Probabilistic precipitation forecasts from a deterministic model: a pragmatic approach, *Meteorol. Appl.*, **12**, 257–268, DOI: 10.1017/S1350482705001763.

Wernli, H., Paulat, M., Hagen, M. and Frei, C. (2008): SAL – A novel quality measure for the verification of quantitative precipitation forecasts, *Mon. Wea. Rev.*, **136**, 4470–4487, DOI: 10.1175/2008MWR2415.1.

WMO (2008): Recommendations for the verification and intercomparison of QPFs and PQPFs from operational NWP models. Revision 2, October 2008, (WMO/TD-No. 1485 WWRP 2009-1), available at http://www.wmo.int/pages/prog/arep/wwrp/new/documents/WWRP2009-1_web_CD.pdf

SAŽETAK

Vefrifikacija prognoza oborine WRF modelom nad Indijom tijekom monsuna 2010.: CRA metoda

Ananda Kumar Das, Mansi Bhowmick, P. K. Kundu i S. K. Roy Bhowmik

Prognoza oborine dobivena modelom WRF za monsunsku sezonu 2010. verificirana je korištenjem analize dnevne opažene oborine u mreži prostorne rezolucije od 0,5°. Određeni su jednostavni, standardni pokazatelji poput srednje pogreške i srednje kvadratne pogreške, a također i dva uobičajena kategorička pokazatelja uspješnosti koji su izračunati za sedam različitih pragova oborine. Ti pokazatelji su omogućili općenitu procjenu uspješnosti modela te su ukazali na smanjenu pouzdanost za kategorije oborine veće od 7,5 mm. Kako bi se detaljnije procijenila uspješnost modela, verifikacija prognoze oborine je također napravljena pomoću objektno orijentirane metode bliskih oborinskih područja CRA (Contiguous Rain Area). Ova metoda je također ukazala na smanjenje uspješnosti modela s povećanjem količine oborine. Međutim, dekompozicija srednje kvadratne pogreške je ukazala da najveću pogrešku uzrokuje pomak prognoziranog oborinskog područja ili događaja u odnosu na izmjerene vrijednosti. Za 24-satne prognoze volumna pogreška doprinosi manje u usporedbi s prostornom pogreškom, neovisno o pragovima oborine. Međutim, za 48-satne prognoze iznosi volumne i prostorne pogreške su usporedivi te rastu s pragom oborine. Susjedna oborinska područja za prognoziranu oborinu su određena obzirom na izmjerenu oborinu primjenom kriterija nabolje podudarnosti. Postupak je proveden za cijelu monsunsku sezonu. Za područja s količinom oborine manjom od 50 mm podudaranje je veće od 70%.

Ključne riječi: susjedno oborinsko područje

Corresponding author's address: Ananda Kumar Das, India Meteorological Department, Mausam Bhawan, Lodi Road, New Delhi, India; phone: +91 11 4382 4481; e-mail: akuda.imd@gmail.com